Optimization of a semianalytical ocean color model for global-scale applications

Stéphane Maritorena, David A. Siegel, and Alan R. Peterson

Semianalytical (SA) ocean color models have advantages over conventional band ratio algorithms in that multiple ocean properties can be retrieved simultaneously from a single water-leaving radiance spectrum. However, the complexity of SA models has stalled their development, and operational implementation as optimal SA parameter values are hard to determine because of limitations in development data sets and the lack of robust tuning procedures. We present a procedure for optimizing SA ocean color models for global applications. The SA model to be optimized retrieves simultaneous estimates for chlorophyll (Chl) concentration, the absorption coefficient for dissolved and detrital materials [$a_{\mathrm{cdm}}(443)$], and the particulate backscatter coefficient [$b_{bp}(443)$] from measurements of the normalized water-leaving radiance spectrum. Parameters for the model are tuned by simulated annealing as the global optimization protocol. We first evaluate the robustness of the tuning method using synthetic data sets, and we then apply the tuning procedure to an *in situ* data set. With the tuned SA parameters, the accuracy of retrievals found with the globally optimized model (the Garver–Siegel–Maritorena model version 1; hereafter GSM01) is excellent and results are comparable with the current Sea-viewing Wide Field-of-view sensor (SeaWiFS) algorithm for Chl. The advantage of the GSM01 model is that simultaneous retrievals of $a_{\mathrm{cdm}}(443)$ and $b_{bp}(443)$ are made that greatly extend the nature of global applications that can be explored. Current limitations and further developments of the model are discussed.

OCIS code: 010.4450.

1. Introduction

Ocean color applications utilize the spectral characteristics and variations of radiometric data to derive information about some of the constituents of the water. Over the past two decades, most efforts were aimed at predicting the concentration of subsurface marine chlorophyll (Chl) a concentration, and this was generally achieved with empirical relationships between reflectance [$R_{rs}(\lambda)$] or, equivalently, normalized water-leaving radiance [$L_{wN}(\lambda)$] and Chl.[1] Since the late 1980s, sophisticated models have been developed[2–8] based on optical closure relationships. These models relate reflectance spectra or $L_{wN}(\lambda)$ to relevant inherent optical properties (IOPs) of seawater, namely, the backscattering $b_b(\lambda)$ and absorption $a(\lambda)$ coefficients. The inversion of the closure formulation thus allows the quantitative assessment of seawater optical characteristics, including the Chl concentration and optical properties. Because the closure relationships contain empirical formulations, these models are generally referred to as semianalytical (SA) models.

Although empirical algorithms are relatively successful for the prediction of Chl in the upper layer of oceanic waters,[1] the SA approach has several benefits. SA models have the most potential of providing accurate retrievals of several parameters simultaneously because they attempt to model the physics of ocean color. As such, they can handle confounding conditions where multiple optical factors control ocean color. Hence these models reflect our current understanding of ocean color. Although not presented here, SA models also have the capability of producing rigorous error estimates and can take into account the uncertainties of incoming data.[5]

The successful development of a SA model requires one to overcome several issues. Although the general expression of optical closure relationships is fairly simple {$R_{rs}(\lambda)$ or $L_{wN}(\lambda) = f[b_b(\lambda)/a(\lambda)]$}, their

S. Maritorena (stephane@icess.ucsb.edu), D. A. Siegel, and A. R. Peterson are with the Institute for Computational Earth System Science, University of California, Santa Barbara, Santa Barbara, California 93106-3060. D. A. Siegel is also with the Department of Geography at the University of California, Santa Barbara.

Received 23 May 2001; revised manuscript received 12 December 2001.

0003-6935/02/152705-10$15.00/0

full formulation includes several terms with specific parameterizations. Moreover, most of these terms are nonlinear and vary on the global scale. A complete SA model thus contains many parameters whose values are critical to determine their predicting ability. In recent years, the absorption coefficient of phytoplankton $a_{ph}(\lambda)$,[9] particulates $a_p(\lambda)$,[9] and pure seawater[10] have been well documented. On the other hand, the spareness of *in situ* data on the backscattering coefficient of particulates $b_{bp}(\lambda)$ and the lack of a predictive knowledge for particle phase function make the parameterization of $b_{bp}(\lambda)$ difficult.[8] Although SA models functionally solve the closure problem, some phenomena that contribute to ocean color are crudely approximated or even not taken into account (e.g., Raman scattering, fluorescence, bidirectional reflectance distribution function). For these various reasons, the development of an accurate SA model is difficult, especially for global application.

A global SA model that achieves good performance for all retrieved parameters is an obtainable goal. In the absence of theoretical breakthroughs, the next generation of SA models can be developed by means of globally optimizing their parameters. Here we adapted a global minimization technique, simulated annealing, for this purpose. The technique is applied to the SA model developed initially by Garver and Siegel.[5] The optimization method is presented first. The performance of the method is evaluated with both synthetic and *in situ* data sets. The accuracy of the Chl retrievals of the optimized model (GSM01 for Garver–Siegel–Maritorena, version 1 is compared with that of the current Sea-viewing Wide Field-of-view Sensor) (SeaWiFS) operational Chl algorithm. Current limitations and further developments of the optimization scheme and the GSM01 model are presented.

2. Inversion Model

Garver and Siegel[5] have developed a SA IOP inversion model validated using *in situ* data from the Sargasso Sea. The details of the model are briefly described below. The functional relationship between $L_{wN}(\lambda)$ and IOPs is taken from Gordon *et al.*[3]:

$$\hat{L}_{wN}(\lambda) = \frac{tF_0(\lambda)}{n_w^2} \sum_{i=1}^{2} g_i \left[\frac{b_b(\lambda)}{b_b(\lambda) + a(\lambda)} \right]^i, \quad (1)$$

where t is the sea–air transmission factor, $F_0(\lambda)$ is the extraterrestrial solar irradiance, and n_w is the index of refraction of the water. The IOP spectra, $a(\lambda)$ and $b_b(\lambda)$, are partitioned into relevant components of seawater backscatter $b_{bw}(\lambda)$ and absorption $a_w(\lambda)$, particulate backscatter $b_{bp}(\lambda)$, phytoplankton absorption $a_{ph}(\lambda)$, and the combined dissolved and detrital particulate absorption coefficients $a_{cdm}(\lambda)$, or

$$b_b(\lambda) = b_{bw}(\lambda) + b_{bp}(\lambda), \quad (2a)$$

$$a(\lambda) = a_w(\lambda) + a_{ph}(\lambda) + a_{cdm}(\lambda). \quad (2b)$$

Values of $a_w(\lambda)$ and $b_{bw}(\lambda)$ are assumed to be known constants.[10,11] The contributions to total absorption by detrital particulates and dissolved materials are considered together as a single term, $a_{cdm}(\lambda)$, because of their similar spectral shapes.[12,13]

The nonwater IOP spectra are then parameterized in terms of a known shape with an unknown magnitude taken from the literature:

$$a_{ph}(\lambda) = \text{Chl}\, a_{ph}^*(\lambda), \quad (3a)$$

$$a_{cdm}(\lambda) = a_{cdm}(\lambda_0)\exp[-S(\lambda - \lambda_0)], \quad (3b)$$

$$b_{bp}(\lambda) = b_{bp}(\lambda_0)(\lambda/\lambda_0)^{-\eta}, \quad (3c)$$

where $a_{ph}^*(\lambda)$ is the Chl a specific absorption coefficient, S is the spectral decay constant for cdm absorption,[14,15] η is the power-law exponent for the particulate backscattering coefficient, and λ_0 is a scaling wavelength (443 nm). For $a_{ph}(\lambda)$, $a_{cdm}(\lambda)$, and $b_{bp}(\lambda)$, the unknown magnitudes are the Chl a concentration, the cdm absorption coefficient $[a_{cdm}(\lambda_0)]$, and the particulate backscatter coefficient $[b_{bp}(\lambda_0)]$, respectively. A complete functional form of the inversion model can be expressed as

$$\hat{L}_{wN}(\lambda) = \frac{tF_0(\lambda)}{n_w^2} \sum_{i=1}^{2} g_i \left\{ \frac{b_{bw}(\lambda) + b_{bp}(\lambda_0)(\lambda/\lambda_0)^{-\eta}}{b_{bw}(\lambda) + b_{bp}(\lambda_0)(\lambda/\lambda_0)^{-\eta} + a_w(\lambda) + \text{Chl}\, a_{ph}^*(\lambda) + a_{cdm}(\lambda_0)\exp[-S(\lambda - \lambda_0)]} \right\}^i. \quad (4)$$

In the model [Eq. (4)], several parameters such as $a_w(\lambda)$, $b_{bw}(\lambda)$, $F_0(\lambda)$, and n_w are or can be considered constants whereas the variations of t and g_i should be small in calm seas with clear sky and fairly high Sun elevation.[3,16] It should be noted that the g_i terms are fitting coefficients from Monte Carlo simulations of an idealized ocean by Gordon.[17] If Eq. (4) is used at first order only (instead of quadratic), the g_1 term can be regarded as the f/Q factor.[18,19] The remaining terms, namely, η, S, Chl, $a_{ph}^*(\lambda)$, $b_{bp}(\lambda_0)$, and $a_{cdm}(\lambda_0)$, are potential unknowns. After a sensitivity analysis on data from Bermuda,[5] the initial implementation of this model used constant values for S and η and a model[2] for $a_{ph}^*(\lambda)$. With this design, only three unknowns [Chl, $a_{cdm}(\lambda_0)$ and $b_{bp}(\lambda_0)$] remained and could be retrieved from $L_{wN}(\lambda)$ data measured for more than three wavelengths. Equation (4) can be restated as $\hat{L}_{wN}(\lambda, \mathbf{\Theta}, \mathbf{\Psi})$ where $\mathbf{\Theta}$ is the vector for the retrieved variables, $\mathbf{\Theta} = [\text{Chl}, a_{cdm}(\lambda_0)$ and $b_{bp}(\lambda_0)]$, and $\mathbf{\Psi}$ is the vector of the model parameters, $\mathbf{\Psi} = [a_{ph}^*(\lambda_1) \ldots a_{ph}^*(\lambda_N), S, \eta]$. The variables to retrieve, $\mathbf{\Theta}$, are obtained by minimization of the

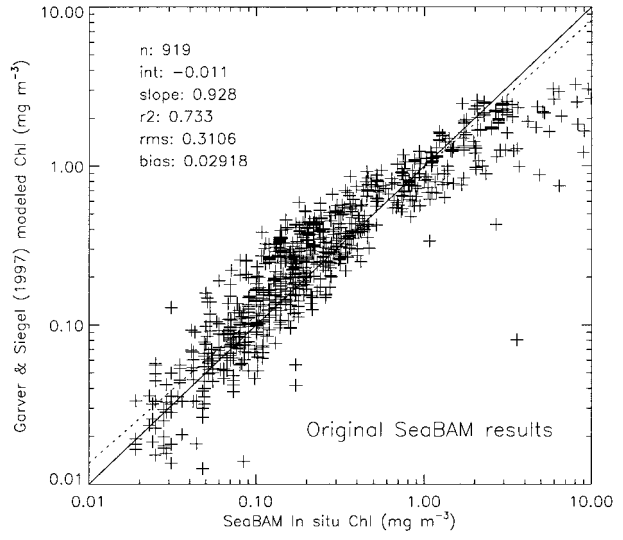

Fig. 1. Chl retrievals of the Garver–Siegel model[5] with its initial set of parameters and the SeaBAM[1] data.

mean square difference (MSD) between modeled and measured $L_{wN}(\lambda)$:

$$\mathrm{MSD} = \frac{1}{(N_\lambda - 1)} \sum_{i=1}^{N_\lambda} [\hat{L}_{wN}(\lambda_i, \boldsymbol{\Theta}, \boldsymbol{\Psi}) - L_{wN}(\lambda_i)]^2, \quad (5)$$

where N_λ is the number of wavelengths available and $L_{wN}(\lambda_i)$ is the measured normalized water-leaving radiance for wavelength i. The Levenberg–Marquardt nonlinear least-squares procedure[20] is used to solve Eq. (4) based on the constraint of Eq. (5). Although not presented here, the procedure allows uncertainty estimates in $L_{wN}(\lambda)$ as well as for the retrieved values to be accounted for.

With this original design, we tested various combinations of the model parameters $\boldsymbol{\Psi}$ using $a_{\mathrm{ph}}{}^*(\lambda)$ formulations and coefficients from the literature and various sets of η and S values.[5,21] Some configurations performed reasonably well although never satisfactorily over the whole Chl range (Fig. 1). This initial version of the model ranked tenth among the 19 algorithms presented in the SeaWiFs Bio-Optical Algorithm Mini-Workshop (SeaBAM) Chl algorithm intercomparison.[1] No intercomparisons were made for the additional products $a_{\mathrm{cdm}}(443)$ and $b_{bp}(443)$. There are various possible reasons for these poor Chl retrievals, including flawed parameterization of some terms (possibly related to the characteristics of the data sets used), limited theoretical knowledge, incorrect or improper simplifying assumptions, or poor quality of the input data. Other aspects that currently hamper the development of SA models are described and discussed in Morel and Maritorena.[8] These difficulties, however, can be circumvented by optimization of the parameters of the model, $\boldsymbol{\Psi}$, so that it achieves the best possible retrievals for Chl $a_{\mathrm{cdm}}(443)$ and $b_{bp}(443)$. This can be considered as a tuning of the model when its parameters are adjusted for typical global conditions.

3. Semianalytical Model Tuning by Simulated Annealing

Optimizing the vector of parameters $\boldsymbol{\Psi}$ to improve the overall performance of the model is not a trivial task because of the large number of (potentially interacting) parameters and because the model is highly nonlinear [Eq. (4)]. To solve this topologically complicated problem, we developed a procedure based on the simulated annealing technique.[20] Compared with other steepest descent minimization techniques that look for the quick and nearby solution, simulated annealing is an iterative heuristic method that permits the search of solutions in the uphill (i.e., lower performance) direction. This allows the system to ultimately find a global minimum. This feature also reduces the importance of the first guesses used to initiate the process that is often a critical aspect of minimization techniques based on the steepest descent methods. Simulated annealing includes three basic elements: (1) a cost function that, given a set of $\boldsymbol{\Psi}$ parameters, evaluates the performance of the model; (2) a candidate generator that randomly proposes new values for the $\hat{\boldsymbol{\Psi}}$ vector, and (3) a decreasing temperature that introduces some randomness in the process and controls its overall progress.

The cost function quantifies the performance of the model for a set of $\boldsymbol{\Psi}$ values produced by the candidate generator. A good cost function must reflect, in a single index, the overall performance for the three retrieved quantities [Chl, $a_{\mathrm{cdm}}(443)$ and $b_{bp}(443)$] that have different orders of magnitude and provide guidance for the realism of $\hat{\boldsymbol{\Psi}}$. A typical formulation of a cost function for this problem is

$$\overline{CF} = \sum_{t=1}^{N_t} \sum_{k=1}^{N_\Theta} \omega_k [\hat{\Theta}_k(\hat{\Psi}; t) - \Theta_k(t)]^2 + \sum_{i=1}^{N_\Psi} \Omega_i [\hat{\Psi}_i - \tilde{\Psi}_i]^2, \quad (6)$$

where N_t is the number of observations, N_Θ is the number of retrieved parameters, $\Theta_k(t)$ represents the *in situ* value of the retrieval, $\hat{\Theta}_k(\hat{\Psi}; t)$ is the model's retrieval for the trial parameter set $\hat{\boldsymbol{\Psi}}$, ω_k quantifies the relative weighting for each derived parameter, N_Ψ is the number of parameters to be optimized, $\tilde{\boldsymbol{\Psi}}$ is the parameter vector of *a priori* guesses, and Ω_i is an *a priori* penalty function. The first summation in Eq. (6) above quantifies the misfit in the retrievals whereas the second summation represents the penalty for the selection of outrageous values in the $\hat{\boldsymbol{\Psi}}$ vector.

We generated candidate $\hat{\boldsymbol{\Psi}}$ vectors using the simplex method.[20,22] A simplex is a N_Ψ-dimensions geometric object defined by $N_\Psi + 1$ points in a N_Ψ-dimensional solution space. The model is evaluated (through the cost function) for each point (vertex) of the simplex that evolves in the solution space by a series of reflections, expansions, or contractions to the worst point of the simplex (highest cost function). This step of moving the worst point of the simplex is

Table 1. Comparison of the Model Parameters (vector Ψ) Used to Create the Synthetic Data Sets and the Values Retrieved by the Simulated Annealing Procedure for the 0, 2, and 5% Noise Data Sets[a]

			Retrieved Values		
Ψ	Units	Exact Values	0% Noise	2% Noise	5% Noise
$a_{ph}^*(412)$	$m^2\ mg^{-1}$	0.0403	0.0397 (1.38)	0.0405 (0.41)	0.0347 (13.84)
$a_{ph}^*(443)$	$m^2\ mg^{-1}$	0.0448	0.0450 (0.52)	0.0439 (1.98)	0.0455 (1.51)
$a_{ph}^*(490)$	$m^2\ mg^{-1}$	0.0312	0.0308 (1.18)	0.0310 (0.16)	0.0261 (16.45)
$a_{ph}^*(510)$	$m^2\ mg^{-1}$	0.0216	0.0210 (2.52)	0.0207 (4.36)	0.0204 (5.62)
$a_{ph}^*(555)$	$m^2\ mg^{-1}$	0.009	0.0089 (1.09)	0.0086 (4.13)	0.0075 (17.01)
S	nm^{-1}	0.015	0.0152 (1.29)	0.0149 (0.35)	0.0179 (19.45)
η	—	1.0	1.0080 (0.82)	1.0080 (0.82)	0.9163 (8.37)

[a]The relative percentage difference is indicated in parentheses ($\Delta\% = |\text{retrieved} - \text{exact}| * 100/\text{exact}$).

repeated until changes in the $\hat{\Psi}$ vector are no longer significant (i.e., when a minimum is reached).

To that point, the procedure works like a classic downhill simplex method.[20] The components that are specific to simulated annealing are the introduction of a random term proportional to a temperature and its associated cooling schedule. The annealing temperature is the parameter that controls the procedure. First, the logarithm of a uniform random deviate (evenly distributed between 0.0 and 1.0) is multiplied by the temperature, and this result is added to the cost function of the simplex points under evaluation. A similar product (with a new random deviate) is subtracted from the replacement points in the simplex. This scheme occasionally allows the selection of an unfavorable solution (uphill step) that enables the optimization procedure to get out of local minima and ultimately find the global minimum. The probability of accepting an unfavorable solution is proportional to the temperature as is the region of the solution space that can be explored by the simplex. During the process, the annealing temperature is slowly reduced at a prescribed cooling rate (cooling schedule). When the temperature approaches zero, the procedure is similar to a downhill simplex method. Simulated annealing is generally considered more reliable than many other optimization schemes with the drawback that it is computationally heavy and time-consuming. It should be mentioned that the computational burden of the procedure is not an issue as the optimization process is conducted only once, the resulting set of parameters being what is always used operationally in the optimized model (GSM01).

In the frame of an SA model, it is necessary that the annealing procedures retrieves parameter values that are within assumed bounds. If the values in the Ψ vector are not constrained, it is possible that the annealing procedure would find a set of parameters that produce excellent agreements between *in situ* data and modeled values but has no fidelity to the underlying physics or biology [such as negative $a_{ph}^*(\lambda)$ values, for example]. The *a priori* penalty term in Eq. (6) is designed to dramatically increase the cost function when elements of the Ψ vector are outside of predefined bounds. However, these bounds must not be too restrictive to allow a meaningful tuning. For example, the low and high bounds for the globally optimized $a_{ph}^*(\lambda)$ were set to 0.005 and 0.3 $m^2\ mg^{-1}$, respectively, at all wavelengths whereas they were set to 0.01 and 0.035 nm^{-1} for S and to 0.0 and 4.3 for η.

4. Testing of the Simulated Annealing Approach with Synthetic Data Sets

The simulated annealing approach was first tested with synthetic data that contained different levels of noise. These tests have several purposes; an obvious one is to validate the implementation of the simulated annealing procedure to see if it performs well. The tests with synthetic data with added noise prefigures how the procedure (and model) may work with real data.

We created synthetic data sets using the model [Eq. (4)] in a forward mode where known values of Chl, $b_{bp}(443)$, and $a_{cdm}(443)$ are used to generate $L_{wN}(\lambda)$ spectra assuming a Ψ vector [following Eq. (4)]. Values for Θ and Ψ were set within realistic ranges and were created from a set of 1000 Chl concentrations uniformly distributed (in log space) between 0.02 and 10.0 mg m^{-3}. The $a_{cdm}(443)$ and $b_{bp}(443)$ terms are parameterized as single power functions of Chl [$a_{cdm}(443) = 0.02*\text{Chl}^{0.2}$ and $b_{bp}(443) = 0.001*\text{Chl}^{0.4}$] with spectral dependence similar to those of Eqs. 3(b) and 3(c), respectively. The $a_{cdm}(\lambda)$ spectral decay constant S was set to 0.015 nm^{-1} whereas η was set to 1.0. For $a_{ph}(\lambda)$, a generic mean $a_{ph}^*(\lambda)$ spectrum[2] was used for $a_{ph}^*(\lambda)$ in a linear function of Chl [$a_{ph}(\lambda) = a_{ph}^*(\lambda)\text{Chl}$]. The Ψ vector is given in Table 1.

In addition, two other synthetic data sets with added noise were also created. Random noise was introduced in the $b_{bp}(\lambda)$ and $a_{cdm}(\lambda)$ spectra before their use in Eq. (4) to generate $L_{wN}(\lambda)$ spectra. Noise was also added to the resulting $L_{wN}(\lambda)$ values. Noise consisted of spectrally uncorrelated normally distributed random deviates with a mean of 1.0 and a standard deviation of 0.02 or 0.05 (referred to, respectively, as the 2% and 5% noise data sets). Whether this scheme reproduces realistic situations does not really matter (see discussion in Gross *et al.*[23]) as these data are designed to assess the tuning procedure and

how it accommodates noisy data. The data sets are identified by a percentage of noise, but it should be kept in mind that the noise introduced is actually frequently higher than this value and that interactions occur between terms with errors in Eq. (4). The 5% noise data set approaches natural variability found *in situ* data. For example, the $R_{rs}(490)/R_{rs}(555)$ ratio in the SeaBAM data set[1] has a coefficient of variation (standard deviation divided by the mean) of 6.48% for Chl values between 0.03 and 0.04 mg m^{-3} whereas the same statistic is equal to 6.99% in the 5% noise data set. Between 0.9 and 1.1 mg m^{-3}, the coefficients of variation for the same ratio are 12.2% and 8.34% for SeaBAM and the 5% noise data sets, respectively.

5. Tuning Results with the Synthetic Data

The simulated annealing procedure was first tested with the three synthetic data sets. All tests were conducted with the first five SeaWiFS bands. Consequently, the simulated annealing procedure must optimize a $\mathbf{\Psi}$ vector with seven elements [five $a_{\mathrm{ph}}^*(\lambda)$ values, S, and η]. Values for the $\mathbf{\Psi}$ vector used to generate the synthetic data set and the relative difference between the initial and the retrieved $\mathbf{\Psi}$ vectors are presented in Table 1. For the data set without added noise, the retrieved parameters are close to the initial values with a maximum difference of 2.52% for $a_{\mathrm{ph}}^*(510)$. These excellent agreements demonstrate that the present approach can solve for the seven unknowns in the complex, nonlinear system of the SA model.

Although the percentage difference between the actual and the retrieved parameters is slightly above 4% for a couple of parameters with the 2% noise synthetic data set (Table 1), the results are good overall with five out of seven parameters estimated with an accuracy better than 2%. For the 5% noise data set, the errors in the retrieved parameters significantly increased (Table 1) for all parameters but did not exceed 20%. It must be kept in mind that the introduction of random noise in the creation of the synthetic data in effect modifies the correct values of $\mathbf{\Psi}$ to be retrieved, so the errors reported for the retrievals are only indicative. Figure 2 shows the modeled versus actual values for Chl, $a_{\mathrm{cdm}}(443)$, and $b_{bp}(443)$ for each of the synthetic data sets when the sets of parameters returned by the annealing procedure are used. The modeled Chl, $a_{\mathrm{cdm}}(443)$, and $b_{bp}(443)$ were retrieved with high fidelity throughout the concentration range even for the 5% noise case. This demonstrates that the annealing procedure can determine reasonably successful parameter candidates even in the presence of significant noise.

6. Development of a Quasi-Real Data Set

Our goal in tuning the SA model is to use it for global applications. Thus it must be tuned by use of observations that represent the global distribution of IOPs and Chl. Unfortunately, to our knowledge, a large data set containing all the quantities required for an objective tuning does not currently exist. During the SeaBAM activity,[1] a large data set with $R_{rs}(\lambda)$ and Chl data was assembled for ocean color algorithm development and testing. Although this data set proved extremely useful to develop the SeaWiFS operational algorithm[1,24] and is widely used within the ocean color community, it cannot be used to tune the model as it lacks the concurrent determinations of $b_{bp}(443)$ and $a_{\mathrm{cdm}}(443)$. Unfortunately, *in situ* backscattering is still rarely measured. Furthermore, $a_{\mathrm{cdm}}(\lambda)$ data are more frequently sampled than $b_{bp}(\lambda)$ but the measurements are not available for much of the SeaBAM data set. It is likely that it will be several years before quality controlled $b_{bp}(\lambda)$ and $a_{\mathrm{cdm}}(\lambda)$ data sets are available for a range of bio-optical provinces.

In the meantime, optical models can be used to estimate the missing $a_{\mathrm{cdm}}(\lambda)$ and $b_{bp}(\lambda)$ estimates in the SeaBAM data set, enabling the development of a complete quasi-real data set. Here, only a cleaned version of the original SeaBAM data with Chl less than 10 mg m^{-3} and assumed to belong to nonpolar case I waters were used.

As described below, existing bio-optical relationships can be used to estimate $a_{\mathrm{cdm}}(443)$ and $b_{bp}(443)$ from Chl data if the diffuse attenuation coefficient is also known at that wavelength. We added the determinations of the diffuse attenuation coefficient at 443 nm, $K_d(443)$, to the SeaBAM data set by querying the SeaWiFS Bio-Optical Archive and Storage System (SeaBASS) archive.[25] However, $K_d(443)$ data were found for only 428 stations. For the remaining stations, $K_d(443)$ was estimated from the Chl determinations according to the diffuse attenuation model presented in Morel and Maritorena.[8] To increase the size of the quasi-real data set, some recent data from the Bermuda Bio-Optics Project[26] and the Plumes and Blooms[27] experiments were added. Also, values of $R_{\mathrm{rs}}(\lambda)$ were converted to $L_{wN}(\lambda)$. This resulted in a data set of 1075 coincident Chl, $L_{wN}(\lambda)$, and $K_d(443)$ determinations.

We derived estimates for $a_{\mathrm{cdm}}(443)$ and $b_{bp}(443)$ data using several bio-optical relationships. First, the scattering coefficient spectrum $b(\lambda)$ is estimated from the *in situ* Chl data by the relationship developed by Loisel and Morel[28], or

$$\begin{aligned} b(\lambda) &= b_w(\lambda) + b_p(\lambda) \\ &= b_w(\lambda) + 0.252\ \mathrm{Chl}^{0.635}(660/\lambda), \end{aligned} \tag{7}$$

where the $b_w(\lambda)$ values are taken from Morel.[11] When we use the equation relating $K_d(443)$ to the absorption and scattering coefficients proposed by Kirk,[29]

$$K_d(443) = [a(443)^2 + 0.256\ a(443)b(443)]^{0.5}, \tag{8}$$

it is possible to solve for the total absorption at 443 nm, $a(443)$, using the $b(\lambda)$ values from Eq. (7) and the $K_d(443)$ data. The $a_{\mathrm{cdm}}(443)$ estimate is then obtained when we subtract water absorption[10] and the

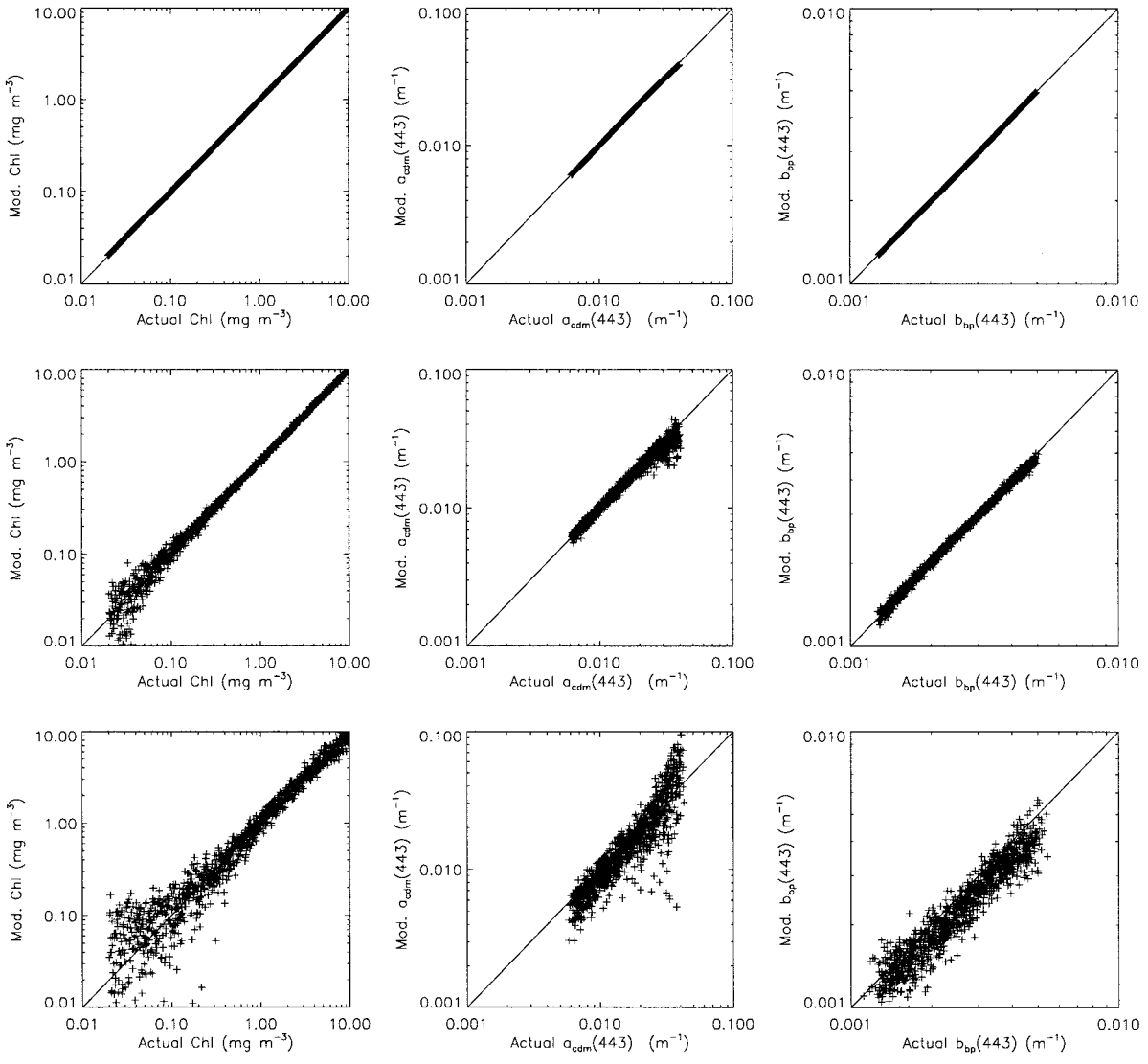

Fig. 2. Retrieved Chl (left panels), $a_{\mathrm{cdm}}(443)$ (center panels), and $b_{bp}(443)$ (right panels) versus the actual values in the synthetic data sets with no noise (upper panels), 2% noise noise (middle panels), and 5% noise (lower panels).

phytoplankton absorption at 443 nm as modeled in Bricaud *et al.*[9] from the total absorption:

$$a_{\mathrm{cdm}}(443) = a(443) - a_w(443) - 0.0365{*}\mathrm{Chl}^{0.615}. \quad (9)$$

Values of $b_{bp}(443)$ are modeled from $b_p(443)$ [right-hand side of Eq. (7)] by use of a backscattering efficiency and a spectral dependence that are both a function of Chl as in Morel and Maritorena.[8] The quasi-real data set is thus composed of 1075 stations containing actual *in situ* measurements for Chl, $L_{wN}(\lambda)$, and derived values for $a_{\mathrm{cdm}}(443)$ and $b_{bp}(443)$. The geometric means for Chl, $a_{\mathrm{cdm}}(443)$, and $b_{bp}(443)$ are 0.578 mg m^{-3}, 0.017 m^{-1}, and 0.0013 m^{-1}, respectively, whereas their respective ranges are 0.023–9.93 mg m^{-3}, 0.0004–0.414 m^{-1}, and 0.00022–0.0099 m^{-1}.

7. Results with the Quasi-Real Data Set

The parameters in the final Ψ vector are presented in Table 2. The optimized $a_{\mathrm{ph}}{*}$ spectrum is plotted (Fig. 3) along with the mean $a_{\mathrm{ph}}{*}$ spectrum used in Morel[2] and a spectrum generated by the Bricaud *et al.*[9] model for a Chl concentration of ~0.35 mg m^{-3}.

Table 2. Selected Set of Optimized Parameters from the Simulated Annealing Procedure Applied to the Quasi-Real Data Set and with the First Five SeaWiFS Bands

Parameter	Ψ
$a_{\mathrm{ph}}{*}(412)$	0.00665
$a_{\mathrm{ph}}{*}(443)$	0.05582
$a_{\mathrm{ph}}{*}(490)$	0.02055
$a_{\mathrm{ph}}{*}(510)$	0.01910
$a_{\mathrm{ph}}{*}(555)$	0.01015
S	0.0206
η	1.0337

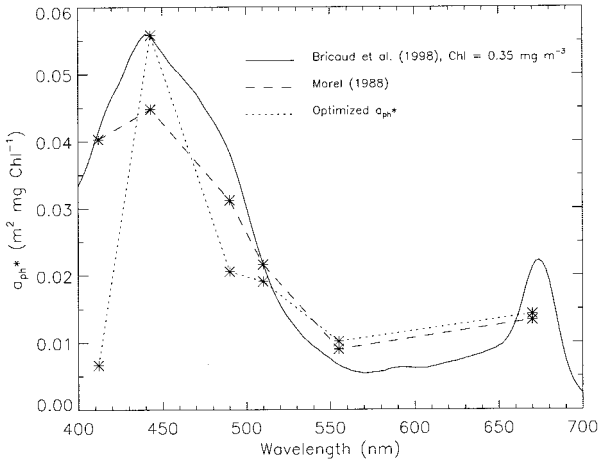

Fig. 3. Comparison of the optimized $a_{ph}^*(\lambda)$ spectrum with the mean spectrum of Morel[2] and a spectrum generated with the model of Bricaud *et al.*[9] for a Chl concentration of 0.35 mg m^{-3}.

Compared with typical $a_{ph}^*(\lambda)$ spectra, the optimized spectrum shows low values at 412 and 490 nm. The low retrieved value of $a_{ph}^*(412)$ may compensate the influence of another parameter at that wavelength, possibly $a_{cdm}(412)$. An S slope of 0.0206 nm^{-1} is consistent with recent observations[13] and is close to the values used by Carder *et al.*[6] and Reynolds *et al.*[7] The exponent of the power law that describes the behavior of the particulate backscattering is slightly above 1 (1.03), which appears to be a typical value.

Retrievals of the globally optimized GSM01 model with the set of parameters produced by the annealing procedure and the quasi-real data set are presented in Fig. 4. For comparison, the Chl retrievals derived with the current operational Chl algorithm of SeaWiFS[24] are also plotted. Both algorithms show excellent agreement between the *in situ* and modeled Chl with no significant difference in the statistics. The optimized model shows no curvature for Chl, and

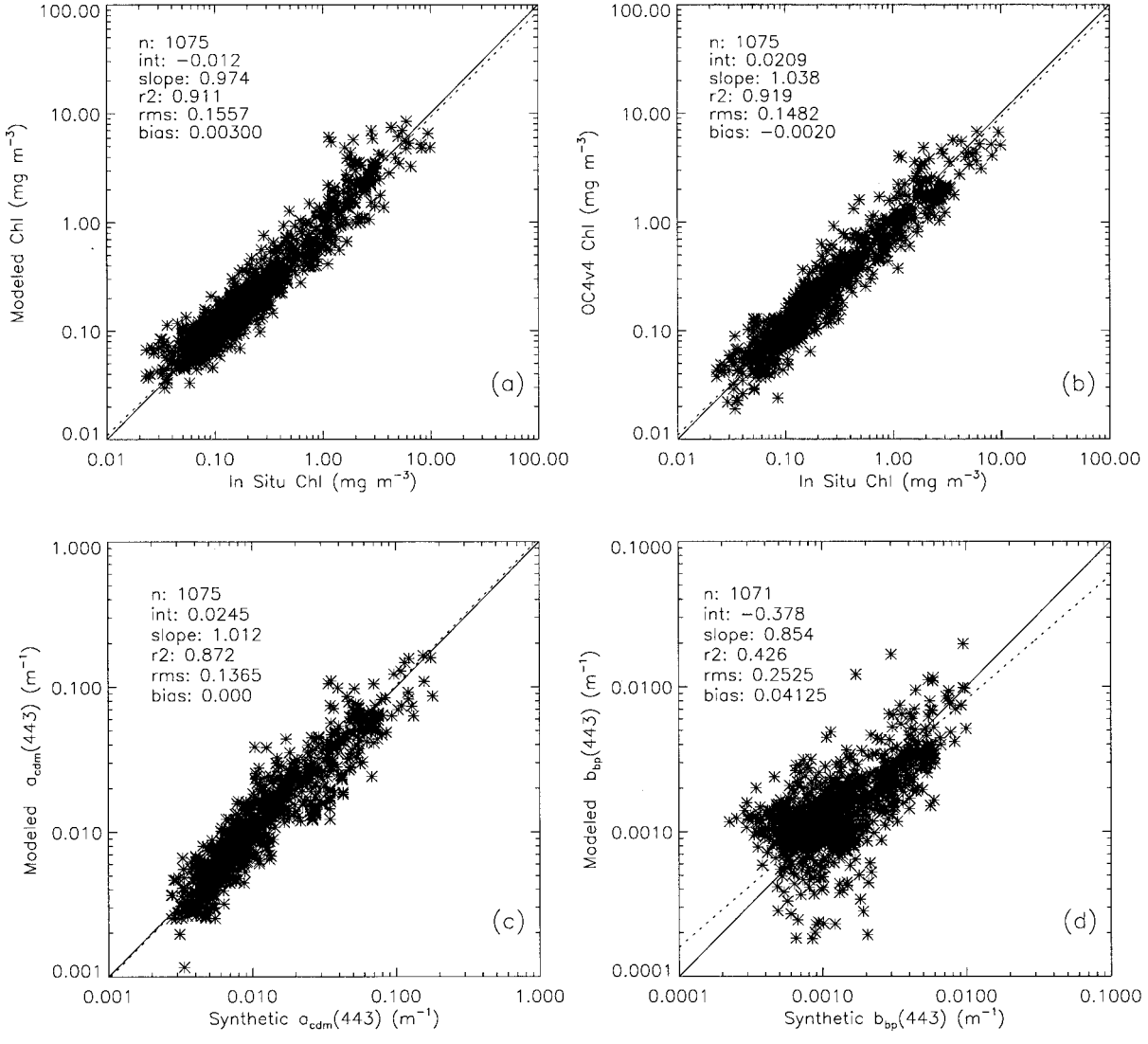

Fig. 4. Results of the GSM01 model with the quasi-real data set by use of the set of parameters selected after the simulated annealing procedure. (a) Chl, (b) Chl estimates with the OC4v4 algorithm,[24] (c) $a_{cdm}(443)$, and (d) $b_{bp}(443)$. For comparison, the original model of Garver and Siegel[5] achieves a slope of 0.876, a r^2 of 0.768, and a rms of 0.333 when used with the quasi-real data set.

the model performs well throughout the concentration range. As addressed above, the GSM01 model also provides independent determinations of important IOP values. After correction for a small offset (0.197 in log space), the $a_{\mathrm{cdm}}(443)$ absorption shows a good agreement between the *in situ* and modeled data (slope of 1.01, $r^2 = 0.87$, Fig. 4). The $b_{bp}(443)$ data are predicted with a bit less fidelity than the other two quantities, possibly because of inconsistencies with the bio-optical models for $b_{bp}(\lambda)$ models.[3,8]

8. Discussion and Conclusions

The overall purpose of this study was to test and present an optimizing scheme that can be used to develop the next generation of SA models so they can be used reliably with *in situ* or satellite ocean color data. Using the original model of Garver and Siegel,[5] we have demonstrated that the performance of a complex nonlinear ocean color model can be significantly improved by application of a global optimization procedure. Use of synthetic data, for which the exact solution is known, demonstrated the ability of the optimization technique to work even in the presence of a substantial amount of noise in the data. For the quasi-real data, the simulated annealing procedure returned parameter values for an optimized model (GSM01) that can estimate Chl with an accuracy similar to that of the current SeaWiFS algorithm. Compared with its original version, the GSM01 model shows a dramatic improvement in terms of the accuracy of the Chl retrievals (Fig. 1 versus Fig. 4).

The Chl concentration is by far the easiest quantity to validate as it is routinely measured. An independent evaluation of the optimized model can be conducted when it is tested for Chl retrievals with data other than that used to tune it. For example, the optimized model has been used with the SeaWiFS match-up data set.[30] This data set contains nearly simultaneous *in situ* and SeaWiFS $L_{wN}(\lambda)$ determinations at the same location (the *in situ* data also include Chl measurements). The match-up data set contains data from various optical provinces and Chl concentrations ranging from ~0.04 to ~5 mg m^{-3}. Use of the optimized model with the *in situ* $L_{wN}(\lambda)$ observations of the match-up data set confirms the good overall behavior [Fig. 5(c)] of the tuned model for Chl retrievals. The improvement over the original model is obvious [Fig. 5(a)], and the statistical performance of GSM01 and OC4v4 [Fig. 5(b)] are virtually identical with a slightly lower bias for the former. The GSM01 model has also been applied to the SeaWiFS imagery[31]; and after evaluation as part of the SeaWiFS data processing at NASA's Goddard Space Flight Center,[32] it was implemented in the SeaWiFS Data Analysis System (SeaDAS) 4.1.[33]

This version of the model should be considered interim because *in situ* $a_{\mathrm{cdm}}(\lambda)$ and $b_{bp}(\lambda)$ data required for the optimization were not available in sufficient amounts but were modeled, and also because the model itself can be refined with further developments. Our primary objective here was to develop

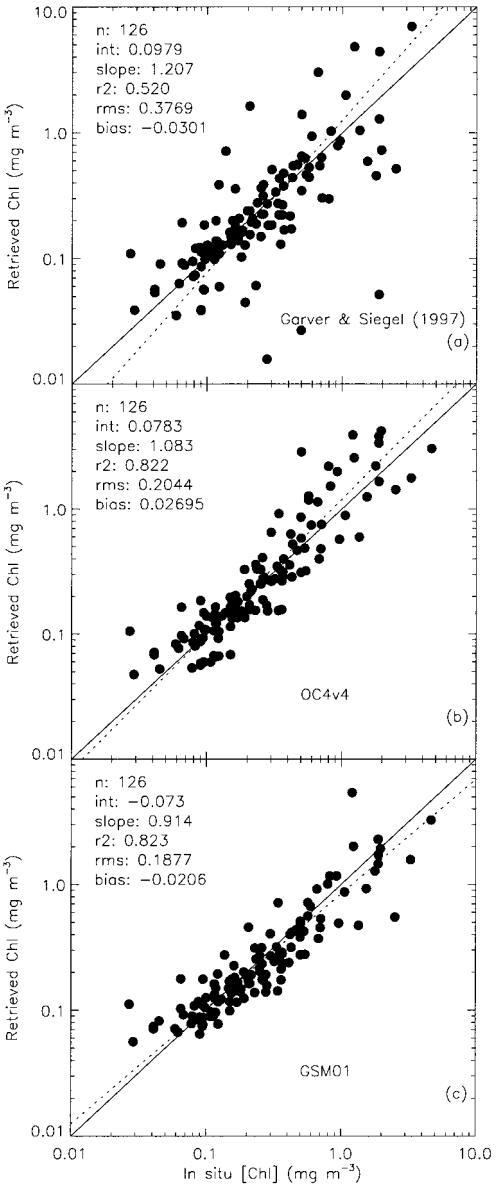

Fig. 5. Chl retrievals generated by the optimized model with the *in situ* $L_{wN}(\lambda)$ data from the SeaWIFS match-up data set versus *in situ* Chl data from that same data set: (a) the original Garver and Siegel model,[5] (b) OC4v4, and (c) the GSM01 model.

the simulated annealing procedure as a general development tool for SA models. As a first step, several components of the model were deliberately formulated by use of simplifying assumptions to limit the number of unknowns the annealing procedure had to solve. This is particularly true for $a_{\mathrm{ph}}^*(\lambda)$ that is here expressed as a constant mean spectrum instead of a more realistic function that may account for photoadaptation or community structure shifts. In the present study, a mean $a_{\mathrm{ph}}^*(\lambda)$ spectrum limits the search of solutions to a seven dimensions space whereas a power-law function of Chl [for example, $a_{\mathrm{ph}}^*(\lambda) = A(\lambda)\ \mathrm{Chl}^{B(\lambda)}$] would extend the search to a 12 dimensions space (14 if the procedure is to solve for six wavelengths). Although time-consuming, the

simulated annealing procedure has the ability to solve for that many unknowns; however, further developments of the model require a formulation of $a_{\mathrm{ph}}^*(\lambda)$ parameterization that have other features than just being realistic in spectral shape and magnitude. For example, in its present form, the model is optimized to work with $L_{wN}(\lambda)$ data at the first five SeaWiFS wavelengths, which obviously limits its general applicability. The main difficulty in making the model more usable with any suite of wavelengths actually comes from the parameterization of $a_{\mathrm{ph}}^*(\lambda)$, as coefficients must be determined for each wavelength. Although it is reasonably straightforward to optimize $a_{\mathrm{ph}}^*(\lambda)$ at five wavelengths, it would be extremely difficult (if not impossible) to do so with many arbitrary wavelengths. It is thus unrealistic to consider an optimized hyperspectral version of the model with the current parameterization for $a_{\mathrm{ph}}^*(\lambda)$. Instead, a formulation that simplifies the spectral description of $a_{\mathrm{ph}}(\lambda)$[34,35] and takes into account its variability with trophic and photoadaptative states can be developed. This would allow a hyperspectral-like behavior without a significant increase in the number of parameters in the model.

The hyperspectral problem does not exist for $a_{\mathrm{cdm}}(\lambda)$ or $b_{bp}(\lambda)$ as their spectral dependence is rather simple and, in addition to S or η, depends only on a single scaling wavelength (λ_0). Although S and η were optimized in our procedure, they are also assumed to be constants in the GSM01 model. It is likely that S and η vary in the world ocean based on the characteristics of the constituents of the water. The equations for $a_{\mathrm{cdm}}(\lambda)$ and $b_{bp}(\lambda)$ [Eqs. 3(b) and 3(c), respectively] can probably be modified to allow these two parameters to vary, possibly as a function of Chl. Although it has some drawbacks, this kind of formulation has already been used for backscattering.[6,8,36] On the other hand, the variations of S in the ocean are more difficult to reproduce as they depend on complex relationships involving the land–sea interactions, the productivity and state of the phytoplankton communities, and the microbial loop and photochemistry.[37] To our knowledge, no clear relationship exists at the global scale between S and any other optical property used in the model. It must also be kept in mind that, in the model, S is a compound value from the dissolved and detrital fractions and that little is known on the individual values of S in each fraction in the world ocean and how they combined to form $a_{\mathrm{cdm}}(\lambda)$.[37]

As mentioned above, the sparseness of concurrent $a_{\mathrm{cdm}}(\lambda)$ and $b_{bp}(\lambda)$ observations did not allow the use of actual measurements. Consequently, a complete validation of the model for these two quantities is still to be performed, although preliminary testing with SeaWiFS imagery seems to indicate a good agreement between independent *in situ* data and the $a_{\mathrm{cdm}}(443)$ values returned by the optimized model.[31] The complete validation of the model for $b_{bp}(443)$ will probably require several years as *in situ* measurements and protocols for *in situ* backscattering measurements are still under development. The optimization procedure presented here clearly improved the performance of the original model. However, in addition to the parameterization issues described above, a full optimization is still hindered by the lack of a fully suited data set. An extensive and complete data set containing $L_{wN}(\lambda)$ and IOP data from around the world's oceans is required to address the issues discussed above. Such effort can be achieved only if investigators from the ocean color community contribute to a global data set. The Sensor Intercomparison and Merger for Biological and Interdisciplinary Studies (SIMBIOS)[38] project would be a good frame for the development of such a data set as, apart from algorithm development, such effort also involves various aspects related to *in situ* measurement protocols, methodologies, and instrumentation.

The authors gratefully acknowledge the support of the NASA SIMBIOS program. We thank Sean Bailey and Jeremy Werdell for their help with the SeaBASS and the SeaWiFS match-up data. We also thank Brian Langston for valuable discussions about the simulated annealing procedure.

References

1. J. E. O'Reilly, S. Maritorena, B. G. Mitchell, D. A. Siegel, K. L. Carder, S. A. Garver, M. Kahru, and C. R. McClain, "Ocean color chlorophyll algorithms for SeaWiFS," J. Geophys. Res. **103** (C11), 24937–24953 (1998).
2. A. Morel, "Optical modeling of the upper ocean in relation to its biogenous matter content (Case I waters), "J. Geophys. Res. **93** (C9), 10749–10768 (1988).
3. H. R. Gordon, O. B. Brown, R. H. Evans, J. W. Brown, R. C. Smith, K. S. Baker, and D. K. Clark, "A semianalytic radiance model of ocean color," J. Geophys. Res. **93** (D9), 10909–10924 (1988).
4. C. S. Roesler and M. J. Perry, "*In situ* phytoplankton absorption, fluorescence emission, and particulate backscattering spectra determined from reflectance," J. Geophys. Res. **100** (C7), 13279–13294 (1995).
5. S. A. Garver and D. A. Siegel, "Inherent optical property inversion of ocean color spectra and its biogeochemical interpretation. I. Time series from the Sargasso Sea," J. Geophys. Res. **102,** 18607–18625 (1997).
6. K. L. Carder, F. R. Chen, Z. P. Lee, S. K. Hawes, and D. Kamykowski, "Semianalytic Moderate-Resolution Imaging Spectrometer algorithms for chlorophyll a and absorption with bio-optical domains based on nitrate-depletion temperatures," J. Geophys. Res. **104** (C3), 5403–5421 (1999).
7. R. A. Reynolds, D. Stramski, and B. G. Mitchell, "A chlorophyll-dependent semianalytical reflectance model derived from field measurements of absorption and backscattering coefficients within the Southern Ocean," J. Geophys. Res. **106** (C4), 7125–7138 (2001).
8. A. Morel and S. Maritorena, "Bio-optical properties of oceanic waters: a reappraisal," J. Geophys. Res. **106** (C4), 7163–7180 (2001).
9. A. Bricaud, A. Morel, M. Babin, K. Allali, and H. Claustre, "Variations of light absorption by suspended particles with chlorophyll a concentration in oceanic (case 1) waters: analysis and implications for bio-optical models," J. Geophys. Res. **103** (C13), 31033–31044 (1998).
10. R. M. Pope and E. S. Fry, "Absorption spectrum (380–700 nm) of pure water. 2. Integrating cavity measurements," Appl. Opt. **36,** 8710–8723 (1997).

11. A. Morel, "Optical properties of pure water and pure sea water," in *Optical Aspects of Oceanography*, N. G. Jerlov and E. S. Nielsen, eds. (Academic, San Diego, Calif., 1974), pp. 1–24.
12. K. L. Carder, S. K. Hawes, K. A. Baker, R. C. Smith, R. G. Steward, and B. G. Mitchell, "Reflectance model for quantifying chlorophyll a in the presence of productivity degradation products," J. Geophys. Res. **96,** 20599–20611 (1991).
13. N. B. Nelson, D. A. Siegel, and A. F. Michaels, "Seasonal dynamics of colored dissolved material in the Sargasso Sea," Deep-Sea Res. I **45,** 931–957 (1998).
14. A. Bricaud, A. Morel, and L. Prieur, "Absorption by dissolved organic matter in the sea (yellow substance) in the UV and visible domains," Limnol. Oceanogr. **26,** 43–53 (1981).
15. S. A. Green and N. V. Blough, "Optical-absorption and fluorescence properties of chromophoric dissolved organic-matter in natural waters," Limnol. Oceanogr **39,** 1903–1916 (1994).
16. R. W. Austin, "Inherent spectral radiance signatures of the ocean surface. Part 2: Ocean color analysis," S. W. Duntley, R. W. Austin, W. H. Wilson, C. F. Edgerton, and S. E. Moran, eds., SIO Ref. 74–10 (Scripps Institution of Oceanography, La Jolla, Calif., 1974).
17. H. R. Gordon, "Ocean color remote sensing: influence of the particle phase function and the solar zenith angle," EOS Trans. Am. Geophys. Union **14,** 1055 (1986).
18. A. Morel and B. Gentili, "Diffuse reflectance of oceanic waters: its dependence on Sun angle as influenced by the molecular scattering contribution," Appl. Opt. **30,** 4427–4438 (1991).
19. A. Morel and B. Gentili, "Diffuse reflectance of oceanic water. II. Bidirectional aspects," Appl. Opt. **32,** 6864–6879 (1993).
20. W. H. Press, S. A. Teukolsky, W. T. Vettering, and B. P. Flannery, *Numerical Recipes in C: The Art of Scientific Computing*, 2nd ed. (Cambridge U. Press, New York, 1992).
21. S. A. Garver, "Variability in ocean color observations and their use in the study of upper ocean ecosystem dynamics," Ph.D. dissertation (University of California, Santa Barbara, Santa Barbara, Calif., 1997).
22. J. A. Nelder and R. Mead, "A simplex method for function minimization," Computer J. **7,** 308–313 (1965).
23. L. Gross, S. Thiria, R. Frouin, and B. G. Mitchell, "Artificial neural networks for modeling the transfer function between marine reflectance and phytoplankton pigment concentration," J. Geophys. Res. **105** (C2), 3483–3495 (2000).
24. J. E. O'Reilly, S. Maritorena, M. C. O'Brien, D. A. Siegel, D. Toole, D. Menzies, R. C. Smith, J. L. Mueller, B. G. Mitchell, M. Kahru, R. P. Chavez, P. Strutton, G. F. Cota, S. B. Hooker, C. R. McClain, K. L. Carder, F. Mueller-Karger, L. Harding, A. Magnusion, D. Phynney, G. F. Moore, J. Aiken, K. R. Arrigo, R. Letelier, and M. Culver, *SeaWiFS Postlaunch Calibration and Validation Analyses, Part 3*, NASA Tech. Memo. 2000-206892, Vol. 11, S. B. Hooker and E. R. Firestone, eds. (NASA Goddard Space Flight Center, Greenbelt, Md., 2000).
25. S. B. Hooker, C. R. McClain, J. K. Firestone, T. L. Westphal, E.-N. Yeh, and Y. Ge, *The SeaWiFS Bio-Optical Archive and Storage System* (*SeaBASS*). *Part 1*, NASA Tech. Memo. 104566, Vol. 20 (NASA Goddard Space Flight Center, Greenbelt, Md., 1994).
26. D. A. Siegel and A. F. Michaels, "Quantification of non-algal light attenuation in the Sargasso Sea: implications for biogeochemistry and remote sensing," Deep-Sea Res. II **43,** 321–345 (1996).
27. D. A. Toole and D. A. Siegel, "Modes and mechanisms of ocean color variability in the Santa Barbara Channel," J. Geophys. Res. **106** (C11), 26985–27000 (2001).
28. H. Loisel and A. Morel, "Light scattering and chlorophyll concentration in case 1 waters: a reexamination," Limnol. Oceanogr. **43,** 847–858 (1998).
29. J. T. O. Kirk, "Monte Carlo study of the nature of the underwater light field in and the relationships between opticals properties of turbid yellow waters," Aust. J. Mar. Freshwater Res. **32,** 517–532 (1981).
30. C. R. McClain, R. A. Barnes, R. E. Eplee, Jr., B. A. Franz, N. C. Hsu, F. S. Patt, C. M. Pietras, W. D. Robinson, B. D. Schieber, G. M. Schmidt, M. Wang, S. W. Bailey, and P. J. Werdell, *SeaWiFS Postlaunch Calibration and Validation Analyses, Part 2*, NASA Tech. Memo. 2000-206892, Vol. 10, S. B. Hooker and E. R. Firestone, eds. (NASA Goddard Space Flight Center, Greenbelt, Md., (2000).
31. D. A. Siegel, S. Maritorena, N. B. Nelson, D. A. Hansell, and M. Lorenzi-Kayser, "Global distribution and dynamics of colored dissolved and detrital organic materials," J. Geophys. Res. (to be published).
32. For further information, see http://seawifs.gsfc.nasa.gov/ cgi-brs/level3.pl.
33. K. Baith, R. Lindsay, G. Fu, and C. R. McClain, "Data analysis system developed for ocean color satellite sensors," EOS Trans. **82,** 202–000 (2001).
34. N. Hoepffner and S. Sathyendranath, "Determination of the major groups of phytoplankton pigments from the absorption-spectra of total particulate matter. J. Geophys. Res. **98** (C12), 22789–22803 (1993).
35. R. Aguirre-Gómez, A. R. Weeks, and S. R. Boxall, "The identification of phytoplankton pigments from absorption spectra," Int. J. Remote Sens. **22,** 315–338 (2001).
36. O. Ulloa, S. Sathyendranath, and T. Platt, "Effect of the particle-size distribution on the backscattering ratio in seawater," Appl. Opt. **33,** 7070–7077 (1994).
37. N. B. Nelson and D. A. Siegel, "Distribution and dynamics of chromophoric dissolved organic matter (CDOM) in the open ocean, in *Biogeochemistry of Marine Dissolved Organic Matter*, D. A. Hansell and C. A. Carlson eds. (Academic, San Diego, Calif., 2002).
38. G. Fargion and C. R. McClain, *SIMBIOS Project 2000 Annual Report*, NASA Tech. Memo. 2001-209976 (NASA Goddard Space Flight Center, Greenbelt, Md., 2001).